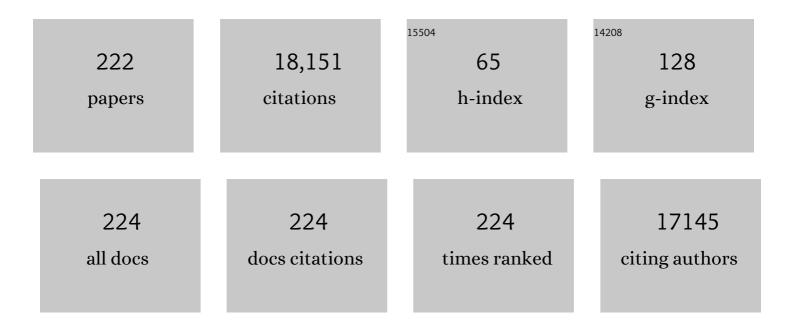
List of Publications by Year in descending order

Source: https://exaly.com/author-pdf/2338159/publications.pdf Version: 2024-02-01



DENC-FELWANC

#	Article	IF	CITATIONS
1	Directional Oxygen Functionalization by Defect in Different Metamorphicâ€Grade Coalâ€Derived Carbon Materials for Sodium Storage. Energy and Environmental Materials, 2022, 5, 313-320.	12.8	30
2	Interfacial Design for a 4.6ÂV Highâ€Voltage Singleâ€Crystalline LiCoO ₂ Cathode. Advanced Materials, 2022, 34, e2108353.	21.0	98
3	Aqueous electrolyte design for super-stable 2.5 V LiMn2O4   Li4Ti5O12 pouch cells. Nature Energ 2022, 7, 186-193.	^y , _{39.5}	122
4	Mitigating the Largeâ€Volume Phase Transition of P2â€Type Cathodes by Synergetic Effect of Multiple Ions for Improved Sodiumâ€Ion Batteries. Advanced Energy Materials, 2022, 12, .	19.5	96
5	Modulating Nonâ€Radiative Deactivation via Acceptor Reconstruction to Expand Highâ€Efficient Red Thermally Activated Delayed Fluorescent Emitters. Advanced Optical Materials, 2022, 10, .	7.3	11
6	A Rational Biphasic Tailoring Strategy Enabling Highâ€Performance Layered Cathodes for Sodiumâ€lon Batteries. Angewandte Chemie - International Edition, 2022, 61, .	13.8	41
7	A Rational Biphasic Tailoring Strategy Enabling Highâ€Performance Layered Cathodes for Sodiumâ€lon Batteries. Angewandte Chemie, 2022, 134, .	2.0	13
8	Iron phthalocyanine-derived nanozyme as dual reactive oxygen species generation accelerator for photothermally enhanced tumor catalytic therapy. Biomaterials, 2022, 284, 121495.	11.4	34
9	New insights to build Na+/vacancy disordering for high-performance P2-type layered oxide cathodes. Nano Energy, 2022, 97, 107207.	16.0	31
10	Low-Cost Al-Doped Layered Cathodes with Improved Electrochemical Performance for Rechargeable Sodium-Ion Batteries. ACS Applied Materials & Interfaces, 2022, 14, 23465-23473.	8.0	11
11	A ratiometric fluorescent probe for detection of γ-glutamyl transpeptidase in blood serum and living cells. Spectrochimica Acta - Part A: Molecular and Biomolecular Spectroscopy, 2022, 278, 121325.	3.9	4
12	Both Interface and Bulk Stable LiNi _{0.5} Mn _{1.5} O ₄ Cathodes for High-Energy Li-Ion Batteries. ACS Applied Energy Materials, 2022, 5, 7582-7589.	5.1	2
13	New Xanthene Dyes with NIRâ€I Emission Beyond 1200Ânm for Efficient Tumor Angiography and Photothermal Therapy. Small, 2022, 18, .	10.0	8
14	Interlocking biphasic chemistry for high-voltage P2/O3 sodium layered oxide cathode. Energy Storage Materials, 2022, 50, 730-739.	18.0	44
15	Fast Interfacial Kinetics for Multivalent Metal Batteries Enabled By Solvation Sheath Reorganization. ECS Meeting Abstracts, 2022, MA2022-01, 123-123.	0.0	0
16	An Inorganicâ€Rich Solid Electrolyte Interphase for Advanced Lithiumâ€Metal Batteries in Carbonate Electrolytes. Angewandte Chemie - International Edition, 2021, 60, 3661-3671.	13.8	317
17	An Inorganicâ€Rich Solid Electrolyte Interphase for Advanced Lithiumâ€Metal Batteries in Carbonate Electrolytes. Angewandte Chemie, 2021, 133, 3705-3715.	2.0	29
18	Innovative strategies of hydrogen peroxide-involving tumor therapeutics. Materials Chemistry Frontiers, 2021, 5, 4474-4501.	5.9	16

#	Article	IF	CITATIONS
19	Achieving high singlet-oxygen generation by applying the heavy-atom effect to thermally activated delayed fluorescent materials. Chemical Communications, 2021, 57, 4902-4905.	4.1	27
20	Amphiphilic confined Pt-based nanocatalysts produced by atomic layer deposition with enhanced catalytic performance for biphasic reactions. Green Chemistry, 2021, 23, 8116-8123.	9.0	11
21	Disulfide-Containing Molecular Sticker Assists Cellular Delivery of DNA Nanoassemblies by Bypassing Endocytosis. CCS Chemistry, 2021, 3, 1178-1186.	7.8	17
22	FacileSynthesis of Anatase TiO ₂ Nanocrystals with Coâ€Exposed{101}, {010}/{100} and [111]â€Facets for EfficientPhotodegradation of Methylene Blue. ChemistrySelect, 2021, 6, 2306-2318.	1.5	3
23	Waterâ€5oluble Organic Nanoparticles with Programable Intermolecular Charge Transfer for NIRâ€II Photothermal Antiâ€Bacterial Therapy. Angewandte Chemie, 2021, 133, 11864-11868.	2.0	16
24	Lithium Metal Batteries Enabled by Synergetic Additives in Commercial Carbonate Electrolytes. ACS Energy Letters, 2021, 6, 1839-1848.	17.4	200
25	<scp>d</scp> -Glucose Isomerization with PAMAM Dendrimers as Environmentally Friendly Catalysts. Journal of Agricultural and Food Chemistry, 2021, 69, 5105-5112.	5.2	11
26	Highâ€Energy Aqueous Sodiumâ€lon Batteries. Angewandte Chemie - International Edition, 2021, 60, 11943-11948.	13.8	100
27	Highâ€Energy Aqueous Sodiumâ€lon Batteries. Angewandte Chemie, 2021, 133, 12050-12055.	2.0	13
28	Ultrasoundâ€Enhanced Selfâ€Exciting Photodynamic Therapy Based on Hypocrellin B. Chemistry - an Asian Journal, 2021, 16, 1221-1224.	3.3	3
29	Selfâ€assembly of Amphiphilic Porphyrins To Construct Nanoparticles for Highly Efficient Photodynamic Therapy. Chemistry - A European Journal, 2021, 27, 11195-11204.	3.3	8
30	Cation-Disordered O3-Na _{0.8} Ni _{0.6} Sb _{0.4} O ₂ Cathode for High-Voltage Sodium-Ion Batteries. ACS Applied Materials & Interfaces, 2021, 13, 32948-32956.	8.0	21
31	Dilute Aqueousâ€Aprotic Hybrid Electrolyte Enabling a Wide Electrochemical Window through Solvation Structure Engineering. Advanced Materials, 2021, 33, e2102390.	21.0	28
32	Stabilizing the framework of SAPO-34 zeolite toward long-term methanol-to-olefins conversion. Nature Communications, 2021, 12, 4661.	12.8	32
33	Boron-doped sodium layered oxide for reversible oxygen redox reaction in Na-ion battery cathodes. Nature Communications, 2021, 12, 5267.	12.8	122
34	Structural insights into the dynamic and controlled multiphase evolution of layered-spinel heterostructured sodium oxide cathode. Cell Reports Physical Science, 2021, 2, 100547.	5.6	23
35	Amphiphilic Diketopyrrolopyrrole Derivatives for Efficient Near-Infrared Fluorescence Imaging and Photothermal Therapy. ACS Omega, 2021, 6, 26575-26582.	3.5	8
36	Realizing high-voltage and ultralong-life supercapacitors by a universal interfacial engineering strategy. Journal of Power Sources, 2021, 510, 230406.	7.8	9

#	Article	IF	CITATIONS
37	High-Efficiency Red-Fluorescent Organic Light-Emitting Diodes with Excellent Color Purity. Journal of Physical Chemistry C, 2021, 125, 1980-1989.	3.1	22
38	Ru ₁ Co <i>_n</i> Single-Atom Alloy for Enhancing Fischer–Tropsch Synthesis. ACS Catalysis, 2021, 11, 1886-1896.	11.2	49
39	Microwave-Heated Graphene Realizes Ultrafast Energy Conversion and Thermal Storage. Energy & Fuels, 2021, 35, 898-904.	5.1	4
40	Two-Channel Space Charge Transfer-Induced Thermally Activated Delayed Fluorescent Materials for Efficient OLEDs with Low Efficiency Roll-Off. ACS Applied Materials & Interfaces, 2021, 13, 49066-49075.	8.0	17
41	Solvation sheath reorganization enables divalent metal batteries with fast interfacial charge transfer kinetics. Science, 2021, 374, 172-178.	12.6	238
42	Probing into the building and evolution of primary hydrocarbon pool species in the process of methanol to olefins over H-ZSM-5 zeolite. Molecular Catalysis, 2021, 516, 111968.	2.0	3
43	Assembly of Silicalite-1 Crystals Like Toy Lego Bricks into One-, Two-, and Three-Dimensional Architectures for Enhancing Its Adsorptive Separation and Catalytic Performances. ACS Applied Materials & Interfaces, 2021, 13, 58085-58095.	8.0	5
44	A novel hypocrellin-based assembly for sonodynamic therapy against glioblastoma. Journal of Materials Chemistry B, 2021, 10, 57-63.	5.8	9
45	High Interfacial-Energy Interphase Promoting Safe Lithium Metal Batteries. Journal of the American Chemical Society, 2020, 142, 2438-2447.	13.7	195
46	Both cationic and anionic redox chemistry in a P2-type sodium layered oxide. Nano Energy, 2020, 69, 104474.	16.0	91
47	Recent advances and prospects of carbon dots in cancer nanotheranostics. Materials Chemistry Frontiers, 2020, 4, 449-471.	5.9	101
48	Boosted photovoltaic performance of indenothiophene-based molecular acceptor <i>via</i> fusing a thiophene. Journal of Materials Chemistry C, 2020, 8, 630-636.	5.5	5
49	Direct Conversion of Syngas into Light Olefins with Low CO ₂ Emission. ACS Catalysis, 2020, 10, 2046-2059.	11.2	77
50	Integrating Multiredox Centers into One Framework for High-Performance Organic Li-Ion Battery Cathodes. ACS Energy Letters, 2020, 5, 224-231.	17.4	59
51	Solidâ€5tate Electrolyte Design for Lithium Dendrite Suppression. Advanced Materials, 2020, 32, e2002741.	21.0	219
52	Recent advances in theranostic agents based on natural products for photodynamic and sonodynamic therapy. View, 2020, 1, 20200090.	5.3	31
53	"Water-in-salt―polymer electrolyte for Li-ion batteries. Energy and Environmental Science, 2020, 13, 2878-2887.	30.8	74
54	A two-photon fluorescent probe for sensitive detection and imaging of γ-glutamyl transpeptidase. Chemical Communications, 2020, 56, 10902-10905.	4.1	22

#	Article	IF	CITATIONS
55	Elucidation of the Jahn-Teller effect in a pair of sodium isomer. Nano Energy, 2020, 77, 105167.	16.0	40
56	Highly Efficient, Red Delayed Fluorescent Emitters with Exothermic Reverse Intersystem Crossing via Hot Excited Triplet States. Journal of Physical Chemistry C, 2020, 124, 20816-20826.	3.1	14
57	In situ tuning of electronic structure of catalysts using controllable hydrogen spillover for enhanced selectivity. Nature Communications, 2020, 11, 4773.	12.8	81
58	Nearâ€Infrared Hypocrellin Derivatives for Synergistic Photodynamic and Photothermal Therapy. Chemistry - an Asian Journal, 2020, 15, 3462-3468.	3.3	12
59	Tuning the Anode–Electrolyte Interface Chemistry for Garnetâ€Based Solidâ€5tate Li Metal Batteries. Advanced Materials, 2020, 32, e2000030.	21.0	156
60	Hypocrellin-Based Multifunctional Phototheranostic Agent for NIR-Triggered Targeted Chemo/Photodynamic/Photothermal Synergistic Therapy against Glioblastoma. ACS Applied Bio Materials, 2020, 3, 3817-3826.	4.6	18
61	Recent advances and prospects of layered transition metal oxide cathodes for sodium-ion batteries. Energy Storage Materials, 2020, 30, 9-26.	18.0	127
62	Realizing Complete Solidâ€Solution Reaction in High Sodium Content P2â€Type Cathode for Highâ€Performance Sodiumâ€Ion Batteries. Angewandte Chemie - International Edition, 2020, 59, 14511-14516.	13.8	142
63	Realizing Complete Solidâ€Solution Reaction in High Sodium Content P2â€Type Cathode for Highâ€Performance Sodiumâ€Ion Batteries. Angewandte Chemie, 2020, 132, 14619-14624.	2.0	65
64	Synthesis of HZSM-5 Rich in Paired Al and Its Catalytic Performance for Propane Aromatization. Catalysts, 2020, 10, 622.	3.5	3
65	Polyanion-type cathode materials for sodium-ion batteries. Chemical Society Reviews, 2020, 49, 2342-2377.	38.1	422
66	Palladium-Catalyzed Cascade Synthesis of Novel Quinolone- Bis(indolyl)methane Hybrids as Promising α-Glucosidase Inhibitors. Synthesis, 2020, 52, 1680-1686.	2.3	4
67	A Highly Reversible, Dendriteâ€Free Lithium Metal Anode Enabled by a Lithiumâ€Fluorideâ€Enriched Interphase. Advanced Materials, 2020, 32, e1906427.	21.0	168
68	Methanol to olefins over H-RUB-13 zeolite: regulation of framework aluminum siting and acid density and their relationship to the catalytic performance. Catalysis Science and Technology, 2020, 10, 1835-1847.	4.1	24
69	A pre-synthetic strategy to construct single ion conductive covalent organic frameworks. Chemical Communications, 2020, 56, 2747-2750.	4.1	29
70	In Situ Copolymerizated Gel Polymer Electrolyte with Cross-Linked Network for Sodium-Ion Batteries. CCS Chemistry, 2020, 2, 589-597.	7.8	18
71	Large-Scale Synthesis of the Stable Co-Free Layered Oxide Cathode by the Synergetic Contribution of Multielement Chemical Substitution for Practical Sodium-Ion Battery. Research, 2020, 2020, 1469301.	5.7	33
72	In Situ Copolymerizated Gel Polymer Electrolyte with Cross-Linked Network for Sodium-Ion Batteries. CCS Chemistry, 2020, 2, 589-597.	7.8	39

#	Article	lF	CITATIONS
73	Experimental Evidence for "Hot Exciton―Thermally Activated Delayed Fluorescence Emitters. Advanced Optical Materials, 2019, 7, 1801190.	7.3	56
74	Facile Formation of Anatase/Rutile TiO2 Nanocomposites with Enhanced Photocatalytic Activity. Molecules, 2019, 24, 2996.	3.8	142
75	Optically tunable fluorescent carbon nanoparticles and their application in fluorometric sensing of copper ions. Nano Research, 2019, 12, 2576-2583.	10.4	47
76	Functionalized Acrylonitriles with Aggregation-Induced Emission: Structure Tuning by Simple Reaction-Condition Variation, Efficient Red Emission, and Two-Photon Bioimaging. Journal of the American Chemical Society, 2019, 141, 15111-15120.	13.7	155
77	Lithiumâ€lon Batteries: Suppressing Manganese Dissolution via Exposing Stable {111} Facets for Highâ€Performance Lithiumâ€lon Oxide Cathode (Adv. Sci. 13/2019). Advanced Science, 2019, 6, 1970076.	11.2	14
78	Deepâ€Red/Nearâ€Infrared Electroluminescence from Singleâ€Component Chargeâ€Transfer Complex via Thermally Activated Delayed Fluorescence Channel. Advanced Functional Materials, 2019, 29, 1903112.	14.9	59
79	Angular-Fused Dithianaphthylquinone Derivative: Selective Synthesis, Thermally Activated Delayed Fluorescence Property, and Application in Organic Light-Emitting Diode. Organic Letters, 2019, 21, 8832-8836.	4.6	11
80	An Ordered Ni ₆ â€Ring Superstructure Enables a Highly Stable Sodium Oxide Cathode. Advanced Materials, 2019, 31, e1903483.	21.0	65
81	Chargeâ€Transfer Complexes: Deepâ€Red/Nearâ€Infrared Electroluminescence from Singleâ€Component Chargeâ€Transfer Complex via Thermally Activated Delayed Fluorescence Channel (Adv. Funct. Mater.) Tj ETQq1	1 047843	149gBT /Over
82	The acidic nature of "NMR-invisible―tri-coordinated framework aluminum species in zeolites. Chemical Science, 2019, 10, 10159-10169.	7.4	78
83	Substrate-induced hydrothermal synthesis of hematite superstructures and their Fischer–Tropsch synthesis performance. New Journal of Chemistry, 2019, 43, 3454-3461.	2.8	6
84	Exploiting Lithiumâ€Depleted Cathode Materials for Solid‣tate Li Metal Batteries. Advanced Energy Materials, 2019, 9, 1901335.	19.5	14
85	Air-Stable and High-Voltage Layered P3-Type Cathode for Sodium-Ion Full Battery. ACS Applied Materials & Interfaces, 2019, 11, 24184-24191.	8.0	58
86	Photosensitizers for Photodynamic Therapy. Advanced Healthcare Materials, 2019, 8, e1900132.	7.6	637
87	Nanostructures and Nanomaterials for Sodium Batteries. , 2019, , 265-312.		1
88	Suppressing Manganese Dissolution via Exposing Stable {111} Facets for Highâ€Performance Lithiumâ€lon Oxide Cathode. Advanced Science, 2019, 6, 1801908.	11.2	41
89	Biodegradable Natural Product-Based Nanoparticles for Near-Infrared Fluorescence Imaging-Guided Sonodynamic Therapy. ACS Applied Materials & Interfaces, 2019, 11, 18178-18185.	8.0	55
90	Pheophytin Derived Nearâ€Infraredâ€Light Responsive Carbon Dot Assembly as a New Phototheranotic Agent for Bioimaging and Photodynamic Therapy. Chemistry - an Asian Journal, 2019, 14, 2162-2168.	3.3	47

#	Article	IF	CITATIONS
91	Synthesis of Anatase TiO ₂ Nanocrystals with Defined Morphologies from Exfoliated Nanoribbons: Photocatalytic Performance and Application in Dyeâ€sensitized Solar Cell. ChemistrySelect, 2019, 4, 4443-4457.	1.5	16
92	An effective LiBO2 coating to ameliorate the cathode/electrolyte interfacial issues of LiNi0.6Co0.2Mn0.2O2 in solid-state Li batteries. Journal of Power Sources, 2019, 426, 242-249.	7.8	54
93	Design of Efficient Exciplex Emitters by Decreasing the Energy Gap Between the Local Excited Triplet (3LE) State of the Acceptor and the Charge Transfer (CT) States of the Exciplex. Frontiers in Chemistry, 2019, 7, 188.	3.6	7
94	A Stable Layered Oxide Cathode Material for Highâ€Performance Sodiumâ€lon Battery. Advanced Energy Materials, 2019, 9, 1803978.	19.5	191
95	High performance low-dimensional perovskite solar cells based on a one dimensional lead iodide perovskite. Journal of Materials Chemistry A, 2019, 7, 8811-8817.	10.3	54
96	Substitution Conformation Balances the Oscillator Strength and Singlet–Triplet Energy Gap for Highly Efficient D–A–D Thermally Activated Delayed Fluorescence Emitters. Advanced Optical Materials, 2019, 7, 1801767.	7.3	29
97	Intermolecular Interaction-Induced Thermally Activated Delayed Fluorescence Based on a Thiochromone Derivative. Journal of Physical Chemistry Letters, 2019, 10, 1888-1893.	4.6	23
98	Extended Electrochemical Window of Solid Electrolytes via Heterogeneous Multilayered Structure for Highâ€Voltage Lithium Metal Batteries. Advanced Materials, 2019, 31, e1807789.	21.0	333
99	Microwave-Assisted Synthesis of High-Energy Faceted TiO2 Nanocrystals Derived from Exfoliated Porous Metatitanic Acid Nanosheets with Improved Photocatalytic and Photovoltaic Performance. Materials, 2019, 12, 3614.	2.9	19
100	The Promotion Effect of Transition Metals on Waterâ€Tolerant Performance of Cu/SiO ₂ Catalysts in Hydrogenation Reaction. ChemistrySelect, 2019, 4, 14063-14068.	1.5	8
101	High efficiency, high color rendering index white organic light-emitting diodes based on thermally activated delayed fluorescence materials. Applied Physics Letters, 2019, 115, .	3.3	9
102	Natural-Origin Hypocrellin-HSA Assembly for Highly Efficient NIR Light-Responsive Phototheranostics against Hypoxic Tumors. ACS Applied Materials & Interfaces, 2019, 11, 44989-44998.	8.0	27
103	A P2/P3 composite layered cathode for high-performance Na-ion full batteries. Nano Energy, 2019, 55, 143-150.	16.0	142
104	Gas phase dehydration of glycerol to acrolein over NaHSO 4 @Zrâ€MCMâ€41 catalyst. Canadian Journal of Chemical Engineering, 2019, 97, 1152-1159.	1.7	2
105	Highly efficient white light-emitting diodes with a bi-component emitting layer based on blue and yellow thermally activated delayed fluorescence emitters. Journal of Materials Chemistry C, 2018, 6, 2951-2956.	5.5	26
106	Effect of Benzene Rings' Incorporation on Photovoltaic Performance of Indacenodithiophene ored Molecular Acceptors. Chinese Journal of Chemistry, 2018, 36, 306-310.	4.9	4
107	Na ⁺ /vacancy disordering promises high-rate Na-ion batteries. Science Advances, 2018, 4, eaar6018.	10.3	341
108	Azo-linked porous organic polymers: robust and time-efficient synthesis <i>via</i> NaBH ₄ -mediated reductive homocoupling on polynitro monomers and adsorption capacity towards aniline in water. Journal of Materials Chemistry A, 2018, 6, 5608-5612.	10.3	36

#	Article	IF	CITATIONS
109	Cancer Therapy: A Magnetofluorescent Carbon Dot Assembly as an Acidic H ₂ O ₂ â€Driven Oxygenerator to Regulate Tumor Hypoxia for Simultaneous Bimodal Imaging and Enhanced Photodynamic Therapy (Adv. Mater. 13/2018). Advanced Materials, 2018, 30, 1870093.	21.0	3
110	Highly Efficient, Solution-Processed Organic Light-Emitting Diodes Based on Thermally Activated Delayed-Fluorescence Emitter with a Mixed Polymer Interlayer. ACS Applied Energy Materials, 2018, 1, 543-551.	5.1	29
111	A Magnetofluorescent Carbon Dot Assembly as an Acidic H ₂ O ₂ â€Driven Oxygenerator to Regulate Tumor Hypoxia for Simultaneous Bimodal Imaging and Enhanced Photodynamic Therapy. Advanced Materials, 2018, 30, e1706090.	21.0	385
112	Trapping Lithium into Hollow Silica Microspheres with a Carbon Nanotube Core for Dendrite-Free Lithium Metal Anodes. Nano Letters, 2018, 18, 297-301.	9.1	130
113	PEGylated carbon dot/MnO2 nanohybrid: a new pH/H2O2-driven, turn-on cancer nanotheranostics. Science China Materials, 2018, 61, 1325-1338.	6.3	44
114	Singlet Oxygen Kinetics in Polymeric Photosensitizers. Journal of Physical Chemistry C, 2018, 122, 12071-12076.	3.1	10
115	An Abnormal 3.7â€Volt O3â€Type Sodiumâ€ion Battery Cathode. Angewandte Chemie, 2018, 130, 8310-8315.	2.0	23
116	An Abnormal 3.7â€Volt O3â€Type Sodiumâ€ion Battery Cathode. Angewandte Chemie - International Edition, 2018, 57, 8178-8183.	13.8	109
117	Relation of Catalytic Performance to the Aluminum Siting of Acidic Zeolites in the Conversion of Methanol to Olefins, Viewed via a Comparison between ZSM-5 and ZSM-11. ACS Catalysis, 2018, 8, 5485-5505.	11.2	148
118	Realizing a highly stable sodium battery with dendrite-free sodium metal composite anodes and O3-type cathodes. Nano Energy, 2018, 48, 369-376.	16.0	99
119	Understanding the structural evolution and Na+ kinetics in honeycomb-ordered O′3-Na3Ni2SbO6 cathodes. Nano Research, 2018, 11, 3258-3271.	10.4	35
120	Dendrite-Free Li-Metal Battery Enabled by a Thin Asymmetric Solid Electrolyte with Engineered Layers. Journal of the American Chemical Society, 2018, 140, 82-85.	13.7	404
121	A novel bismuth-based anode material with a stable alloying process by the space confinement of an <i>in situ</i> conversion reaction for a rechargeable magnesium ion battery. Chemical Communications, 2018, 54, 1714-1717.	4.1	42
122	Layered Oxide Cathodes for Sodiumâ€lon Batteries: Phase Transition, Air Stability, and Performance. Advanced Energy Materials, 2018, 8, 1701912.	19.5	519
123	A large-bandgap small-molecule electron acceptor utilizing a new indacenodibenzothiophene core for organic solar cells. Materials Chemistry Frontiers, 2018, 2, 136-142.	5.9	18
124	Micropore blocked core–shell ZSM-22 designed <i>via</i> epitaxial growth with enhanced shape selectivity and high <i>n</i> -dodecane hydroisomerization performance. Catalysis Science and Technology, 2018, 8, 6407-6419.	4.1	23
125	Interface Exciplex Anchoring the Color Stability of Solutionâ€Processed Thermally Activated Delayed Fluorescent White Organic Lightâ€Emitting Diodes. Advanced Optical Materials, 2018, 6, 1800978.	7.3	34
126	Crystallization Mechanism of Pure-Silica ZSM-22 in the Seed-Assistant System. Crystal Growth and Design, 2018, 18, 6591-6601.	3.0	19

#	Article	IF	CITATIONS
127	Biodegradable hypocrellin derivative nanovesicle as a near-infrared light-driven theranostic for dually photoactive cancer imaging and therapy. Biomaterials, 2018, 185, 133-141.	11.4	54
128	Advanced P2-Na _{2/3} Ni _{1/3} Mn _{7/12} Fe _{1/12} O ₂ Cathode Material with Suppressed P2–O2 Phase Transition toward High-Performance Sodium-Ion Battery. ACS Applied Materials & Interfaces, 2018, 10, 34272-34282.	8.0	127
129	Fe2O3 hollow microspheres as highly selective catalysts for the production of $\hat{1}\pm$ -olefins. New Journal of Chemistry, 2018, 42, 17923-17930.	2.8	4
130	Dehydration of Castor Oil over a NaHSO ₄ /MCMâ€41 Catalyst Prepared by Supercritical Impregnation. Chemical Engineering and Technology, 2018, 41, 2186-2195.	1.5	7
131	A Layered–Tunnel Intergrowth Structure for Highâ€Performance Sodiumâ€Ion Oxide Cathode. Advanced Energy Materials, 2018, 8, 1800492.	19.5	116
132	Mitigating Interfacial Potential Drop of Cathode–Solid Electrolyte via Ionic Conductor Layer To Enhance Interface Dynamics for Solid Batteries. Journal of the American Chemical Society, 2018, 140, 6767-6770.	13.7	192
133	New detection method for nucleoside triphosphates based on carbon dots: The distance-dependent singlet oxygen trapping. Analytica Chimica Acta, 2018, 1031, 145-151.	5.4	10
134	Coumarin/fluorescein-fused fluorescent dyes for rapidly monitoring mitochondrial pH changes in living cells. Spectrochimica Acta - Part A: Molecular and Biomolecular Spectroscopy, 2018, 204, 590-597.	3.9	31
135	Insights into the Improved High-Voltage Performance of Li-Incorporated Layered Oxide Cathodes for Sodium-Ion Batteries. CheM, 2018, 4, 2124-2139.	11.7	128
136	In situ X-ray diffraction and thermal analysis of LiNi0.8Co0.15Al0.05O2 synthesized via co-precipitation method. Journal of Energy Chemistry, 2018, 27, 1655-1660.	12.9	29
137	Ameliorating the Interfacial Problems of Cathode and Solidâ€State Electrolytes by Interface Modification of Functional Polymers. Advanced Energy Materials, 2018, 8, 1801528.	19.5	127
138	Dehydration of castor oil over H6P2W18O62@MCM-41. Reaction Kinetics, Mechanisms and Catalysis, 2018, 125, 1007-1021.	1.7	0
139	Gas phase dehydration of glycerol to acrolein on an amino siloxane-functionalized MCM-41 supported Wells–Dawson type H ₆ P ₂ W ₁₈ O ₆₂ catalyst. New Journal of Chemistry, 2018, 42, 14271-14280.	2.8	19
140	Synthesis of carbon dots from Hypocrella bambusae for bimodel fluorescence/photoacoustic imaging-guided synergistic photodynamic/photothermal therapy of cancer. Journal of Colloid and Interface Science, 2018, 526, 302-311.	9.4	105
141	Exposing {010} Active Facets by Multiple‣ayer Oriented Stacking Nanosheets for Highâ€Performance Capacitive Sodiumâ€Ion Oxide Cathode. Advanced Materials, 2018, 30, e1803765.	21.0	142
142	Constructing a Stable Lithium Metal–Gel Electrolyte Interface for Quasi-Solid-State Lithium Batteries. ACS Applied Materials & Interfaces, 2018, 10, 30065-30070.	8.0	45
143	Carbon Dots as Multifunctional Phototheranostic Agents for Photoacoustic/Fluorescence Imaging and Photothermal/Photodynamic Synergistic Cancer Therapy. Advanced Therapeutics, 2018, 1, 1800077.	3.2	77
144	Polymer Dots as Effective Phototheranostic Agents. Photochemistry and Photobiology, 2018, 94, 916-934.	2.5	40

#	Article	IF	CITATIONS
145	Designing High-Performance Composite Electrodes for Vanadium Redox Flow Batteries: Experimental and Computational Investigation. ACS Applied Materials & amp; Interfaces, 2018, 10, 22381-22388.	8.0	42
146	Valorization of Furfural Residue by Hydrothermal Carbonization: Processing Optimization, Chemical and Structural Characterization. ChemistrySelect, 2017, 2, 583-590.	1.5	7
147	Novel P2-type Na _{2/3} Ni _{1/6} Mg _{1/6} Ti _{2/3} O ₂ as an anode material for sodium-ion batteries. Chemical Communications, 2017, 53, 1957-1960.	4.1	43
148	Coumarin-Based Boron Complexes with Aggregation-Induced Emission. Journal of Organic Chemistry, 2017, 82, 3456-3462.	3.2	58
149	Water-Soluble Polythiophene for Two-Photon Excitation Fluorescence Imaging and Photodynamic Therapy of Cancer. ACS Applied Materials & Interfaces, 2017, 9, 14590-14595.	8.0	49
150	Prussian blue nanocubes as cathode materials for aqueous Na-Zn hybrid batteries. Journal of Power Sources, 2017, 355, 18-22.	7.8	109
151	Excellent Comprehensive Performance of Naâ€Based Layered Oxide Benefiting from the Synergetic Contributions of Multimetal Ions. Advanced Energy Materials, 2017, 7, 1700189.	19.5	82
152	Two-photon-excited near-infrared emissive carbon dots as multifunctional agents for fluorescence imaging and photothermal therapy. Nano Research, 2017, 10, 3113-3123.	10.4	246
153	Dehydration of Castor Oil over NaHSO ₄ /MCMâ€41 Catalyst Modified by <i>n</i> â€Dodecyltriethoxysilane. Zeitschrift Fur Anorganische Und Allgemeine Chemie, 2017, 643, 772-779.	1.2	8
154	Highâ€Energy/Power and Lowâ€Temperature Cathode for Sodiumâ€Ion Batteries: In Situ XRD Study and Superior Fullâ€Cell Performance. Advanced Materials, 2017, 29, 1701968.	21.0	350
155	Biocompatible Iron Phthalocyanine–Albumin Assemblies as Photoacoustic and Thermal Theranostics in Living Mice. ACS Applied Materials & Interfaces, 2017, 9, 21124-21132.	8.0	59
156	Designing Air-Stable O3-Type Cathode Materials by Combined Structure Modulation for Na-Ion Batteries. Journal of the American Chemical Society, 2017, 139, 8440-8443.	13.7	303
157	Dualâ€Emission Channels for Simultaneous Sensing of Cysteine and Homocysteine in Living Cells. Chemistry - an Asian Journal, 2017, 12, 2098-2103.	3.3	21
158	Selfâ€Assembled Carbon Dot Nanosphere: A Robust, Nearâ€Infrared Lightâ€Responsive, and Vein Injectable Photosensitizer. Advanced Healthcare Materials, 2017, 6, 1601419.	7.6	41
159	Versatile Polymer Nanoparticles as Twoâ€Photonâ€Triggered Photosensitizers for Simultaneous Cellular, Deepâ€Tissue Imaging, and Photodynamic Therapy. Advanced Healthcare Materials, 2017, 6, 1601431.	7.6	35
160	Ti‧ubstituted NaNi _{0.5} Mn _{0.5â€} <i>_x</i> Ti <i>_x</i> O ₂ Cathodes with Reversible O3â^P3 Phase Transition for Highâ€Performance Sodiumâ€Ion Batteries. Advanced Materials, 2017, 29, 1700210.	21.0	309
161	Near-Infrared Probe Based on Rhodamine Derivative for Highly Sensitive and Selective Lysosomal pH Tracking. Analytical Chemistry, 2017, 89, 1922-1929.	6.5	134
162	Ethylene glycol-mediated synthetic route for production of luminescent silicon nanorod as photodynamic therapy agent. Science China Materials, 2017, 60, 881-891.	6.3	10

PENG-FEI WANG

#	Article	IF	CITATIONS
163	Triplet decay-induced negative temperature dependence of the transient photoluminescence decay of thermally activated delayed fluorescence emitter. Journal of Materials Chemistry C, 2017, 5, 12077-12084.	5.5	48
164	Honeycomb-Ordered Na ₃ Ni _{1.5} M _{0.5} BiO ₆ (M = Ni, Cu,) Tj ETG 2715-2722.	Qq0 0 0 rg 17.4	BT /Overlock 70
165	Iron oxyfluorides as lithium-free cathode materials for solid-state Li metal batteries. Journal of Materials Chemistry A, 2017, 5, 18464-18468.	10.3	16
166	High-Thermal- and Air-Stability Cathode Material with Concentration-Gradient Buffer for Li-Ion Batteries. ACS Applied Materials & Interfaces, 2017, 9, 42829-42835.	8.0	74
167	n-Doping-induced efficient electron-injection for high efficiency inverted organic light-emitting diodes based on thermally activated delayed fluorescence emitter. Journal of Materials Chemistry C, 2017, 5, 8400-8407.	5.5	29
168	A fluorescent probe for the efficient discrimination of Cys, Hcy and GSH based on different cascade reactions. Biosensors and Bioelectronics, 2017, 90, 117-124.	10.1	110
169	The effect of adsorbed chromium on the pyrolysis behavior of brown coal and the recovery of chromium. Journal of Thermal Analysis and Calorimetry, 2017, 128, 513-522.	3.6	5
170	Highly Conductive, Air‣table Silver Nanowire@Iongel Composite Films toward Flexible Transparent Electrodes. Advanced Materials, 2016, 28, 7167-7172.	21.0	203
171	Investigation of biological cell–small molecule interactions with a gold surface plasmon resonance sensor using a laser scanning confocal imaging-surface plasmon resonance system. RSC Advances, 2016, 6, 65930-65935.	3.6	3
172	Suppressing the P2–O2 Phase Transition of Na _{0.67} Mn _{0.67} Ni _{0.33} O ₂ by Magnesium Substitution for Improved Sodiumâ€ion Batteries. Angewandte Chemie - International Edition, 2016, 55, 7445-7449.	13.8	439
173	Carbon Dots with Intrinsic Theranostic Properties for Bioimaging, Redâ€Lightâ€Triggered Photodynamic/Photothermal Simultaneous Therapy In Vitro and In Vivo. Advanced Healthcare Materials, 2016, 5, 665-675.	7.6	246
174	Ketoâ€benzo[<i>h</i>]â€Coumarinâ€Based Nearâ€Infrared Dyes with Large Stokes Shifts for Bioimaging Applications. Chemistry - an Asian Journal, 2016, 11, 498-504.	3.3	34
175	Zeolite CAN and AFI-Type Zeolitic Imidazolate Frameworks with Large 12-Membered Ring Pore Openings Synthesized Using Bulky Amides as Structure-Directing Agents. Journal of the American Chemical Society, 2016, 138, 16232-16235.	13.7	50
176	Deep-red to near-infrared fluorescent dyes: Synthesis, photophysical properties, and application in cell imaging. Spectrochimica Acta - Part A: Molecular and Biomolecular Spectroscopy, 2016, 164, 8-14.	3.9	15
177	Methane formation mechanism in the initial methanol-to-olefins process catalyzed by SAPO-34. Catalysis Science and Technology, 2016, 6, 5526-5533.	4.1	43
178	Conversion of Methanol to Olefins over H-ZSM-5 Zeolite: Reaction Pathway Is Related to the Framework Aluminum Siting. ACS Catalysis, 2016, 6, 7311-7325.	11.2	285
179	Deep-Red and Near-Infrared Xanthene Dyes for Rapid Live Cell Imaging. Journal of Organic Chemistry, 2016, 81, 7393-7399.	3.2	43

Theranostics: Carbon Dots with Intrinsic Theranostic Properties for Bioimaging, Red-Light-Triggered Photodynamic/Photothermal Simultaneous Therapy In Vitro and In Vivo (Adv. Healthcare Mater.) Tj ETQq0 0 0 rgBT7@verlock110 Tf 50 5 180

#	Article	IF	CITATIONS
181	Surface-enhanced Raman scattering substrate based on cysteamine-modified gold nanoparticle aggregation for highly sensitive pentachlorophenol detection. RSC Advances, 2016, 6, 85285-85292.	3.6	13
182	Highly Efficient Nondoped Organic Light Emitting Diodes Based on Thermally Activated Delayed Fluorescence Emitter with Quantum-Well Structure. ACS Applied Materials & Interfaces, 2016, 8, 20955-20961.	8.0	32
183	A Versatile and Clearable Nanocarbon Theranostic Based on Carbon Dots and Gadolinium Metallofullerene Nanocrystals. Advanced Healthcare Materials, 2016, 5, 2283-2294.	7.6	26
184	A macromolecular cyclometalated gold(<scp>iii</scp>) amphiphile displays long-lived emissive excited state in water: self-assembly and in vitro photo-toxicity. Chemical Communications, 2016, 52, 13273-13276.	4.1	22
185	An O3-type NaNi _{0.5} Mn _{0.5} O ₂ cathode for sodium-ion batteries with improved rate performance and cycling stability. Journal of Materials Chemistry A, 2016, 4, 17660-17664.	10.3	185
186	Suppressing the P2–O2 Phase Transition of Na _{0.67} Mn _{0.67} Ni _{0.33} O ₂ by Magnesium Substitution for Improved Sodiumâ€ion Batteries. Angewandte Chemie, 2016, 128, 7571-7575.	2.0	84
187	Highly efficient inverted organic light-emitting diodes based on thermally activated delayed fluorescence. Science China Materials, 2016, 59, 421-426.	6.3	14
188	Graphene quantum dots as efficient, metal-free, visible -light-active photocatalysts. Science China Materials, 2016, 59, 12-19.	6.3	44
189	A ratiometric fluorescent probe for quantification of alkaline phosphatase in living cells. RSC Advances, 2016, 6, 32046-32051.	3.6	42
190	DOSY NMR: A Versatile Analytical Chromatographic Tool for Lignocellulosic Biomass Conversion. ACS Sustainable Chemistry and Engineering, 2016, 4, 1193-1200.	6.7	30
191	Tunable multicolor carbon dots prepared from well-defined polythiophene derivatives and their emission mechanism. Nanoscale, 2016, 8, 729-734.	5.6	176
192	Light-Emitting Diodes: Highly Efficient Orange and Red Phosphorescent Organic Light-Emitting Diodes with Low Roll-Off of Efficiency using a Novel Thermally Activated Delayed Fluorescence Material as Host (Adv. Mater. 27/2015). Advanced Materials, 2015, 27, 4104-4104.	21.0	1
193	Redâ€Emissive Carbon Dots for Fluorescent, Photoacoustic, and Thermal Theranostics in Living Mice. Advanced Materials, 2015, 27, 4169-4177.	21.0	758
194	Highly Efficient Orange and Red Phosphorescent Organic Lightâ€Emitting Diodes with Low Rollâ€Off of Efficiency using a Novel Thermally Activated Delayed Fluorescence Material as Host. Advanced Materials, 2015, 27, 4041-4047.	21.0	127
195	Controlled cyclic drug release based on chemomechanical gels. Journal of Controlled Release, 2015, 213, e33.	9.9	1
196	Imaging of nucleolar RNA in living cells using a highly photostable deep-red fluorescent probe. Biosensors and Bioelectronics, 2015, 68, 189-196.	10.1	65
197	Catalytic properties and deactivation behavior of H-MCM-22 in the conversion of methanol to hydrocarbons. RSC Advances, 2015, 5, 28794-28802.	3.6	27
198	Nonvolatile memory devices based on carbon nano-dot doped poly(vinyl alcohol) composites with low operation voltage and high ON/OFF ratio. RSC Advances, 2015, 5, 26886-26890.	3.6	16

#	Article	IF	CITATIONS
199	Multifunctional upconversion–nanoparticles–trismethylpyridylporphyrin–fullerene nanocomposite: a near-infrared light-triggered theranostic platform for imaging-guided photodynamic therapy. NPG Asia Materials, 2015, 7, e205-e205.	7.9	84
200	White organic light emitting diodes based on a yellow thermally activated delayed fluorescent emitter. RSC Advances, 2015, 5, 59137-59141.	3.6	16
201	Green Synthesis of Bifunctional Fluorescent Carbon Dots from Garlic for Cellular Imaging and Free Radical Scavenging. ACS Applied Materials & Interfaces, 2015, 7, 17054-17060.	8.0	494
202	A facile high-speed vibration milling method to mass production of water-dispersible silicon quantum dots for long-term cell imaging. RSC Advances, 2015, 5, 35291-35296.	3.6	14
203	Chromogenic/Fluorogenic Ensemble Chemosensing Systems. Chemical Reviews, 2015, 115, 7893-7943.	47.7	351
204	Aminobenzofuran-Fused Rhodamine Dyes with Deep-Red to Near-Infrared Emission for Biological Applications. Journal of Organic Chemistry, 2015, 80, 3170-3175.	3.2	40
205	Deep-Red Emissive Crescent-Shaped Fluorescent Dyes: Substituent Effect on Live Cell Imaging. ACS Applied Materials & Interfaces, 2015, 7, 7421-7427.	8.0	44
206	Highly stable organic fluorescent nanorods for living-cell imaging. Nano Research, 2015, 8, 2380-2389.	10.4	49
207	A selective fluorescent and colorimetric dual-responses chemosensor for streptomycin based on polythiophene derivative. Spectrochimica Acta - Part A: Molecular and Biomolecular Spectroscopy, 2015, 136, 871-874.	3.9	18
208	A graphene quantum dot photodynamic therapy agent with high singlet oxygen generation. Nature Communications, 2014, 5, 4596.	12.8	1,141
209	Investigation of biological cell–protein interactions using SPR sensor through laser scanning confocal imaging–surface plasmon resonance system. Spectrochimica Acta - Part A: Molecular and Biomolecular Spectroscopy, 2014, 121, 381-386.	3.9	20
210	1,4-Diazobicyclo(2,2,2)octane-modified multi-ammonium derivatives as ratiometric fluorescent sensors for lipopolysaccharide. Supramolecular Chemistry, 2013, 25, 69-78.	1.2	3
211	Real time detection of antibody-antigen interaction using a laser scanning confocal imaging-surface plasmon resonance system. Chinese Physics B, 2012, 21, 020601.	1.4	8
212	Synthesis and characterization of cyano-substituted pyridine derivatives for applications as exciton blockers in photovoltaic devices. Journal of Materials Chemistry, 2012, 22, 5107.	6.7	14
213	Bipolar cyano-substituted pyridine derivatives for applications in organic light-emitting devices. Journal of Materials Chemistry, 2012, 22, 8922.	6.7	24
214	Modified silicon nanowires: a fluorescent nitric oxide biosensor with enhanced selectivity and stability. Journal of Materials Chemistry, 2012, 22, 3348.	6.7	19
215	A facile assay for direct colorimetric visualization of lipopolysaccharides at low nanomolar level. Nano Research, 2012, 5, 486-493.	10.4	54
216	A novel fluorogenic hybrid material for selective sensing of thiophenols. Journal of Materials Chemistry, 2011, 21, 13561.	6.7	51

#	ARTICLE	IF	CITATIONS
217	Synthesis and properties of n-type triphenylpyridine derivatives and applications in deep-blue organic light-emitting devices as electron-transporting layer. Journal of Materials Chemistry, 2011, 21, 12977.	6.7	29
218	Aggregation-induced emission enhancement materials with large red shifts and their self-assembled crystal microstructures. CrystEngComm, 2011, 13, 4617.	2.6	31
219	Highly efficient nondoped green organic light-emitting devices based on a substituted triphenylpyridine derivative. Applied Physics Letters, 2009, 95, 133301.	3.3	17
220	Fluorescence chemosensors with pyrene and their interaction with nucleotide phosphate. Science in China Series B: Chemistry, 1999, 42, 236-244.	0.8	2
221	Hyperpolarisability of (donor)2-acceptorâ€type molecules determined by EFISHG. Advanced Materials for Optics and Electronics, 1996, 6, 233-238.	0.4	24
222	Red Fluorescent Organic Light-Emitting Diodes with Low-Efficiency Roll-Off. Energy & Fuels, 0, , .	5.1	3